Electronic Supplementary Material (ESI) for Journal of Materials Chemistry A.
This journal is © The Royal Society of Chemistry 2019

Electronic Supplementary Information

Boosting the Hydrogen Evolution Performance of Ternary $Mo_xCo_{1-x}P$ Nanowire Array by Tuning the Mo/Co Ratio

Yintong Zhang [a], Zhiyuan Wang [g], Feng Du [a], Huichao He [c], Ahmed Alsaedi[h], Tasawar Hayat [h, i], Tao Li [*b], Guo-Ling Li [*g], Yong Zhou [*a, d, f] and Zhigang Zou [a, d, e, f]

[a] *National Laboratory of Solid State Microstructures, Collaborative Innovation Center of Advanced Microstructures, School of Physics, Nanjing University, Nanjing 210093,PR China*

[b] *Engineering Technology Research Center of Henan Province for Solar Catalysis, School of Chemistry and Pharmaceutical Engineering, Nanyang Normal University, Nanyang, Henan, 473061, PR China*

[c] *State Key Laboratory of Environmental Friendly Energy Materials, School of Materials Science and Engineering, Southwest University of Science and Technology, Mianyang, Sichuan 621010, P. R. China*

[d] *Jiangsu Key Laboratory for Nano Technology, Nanjing University, Nanjing 210093, PR China*

[e] *College of Engineering and Applied Sciences, Nanjing University, Nanjing 210093, P. R. China*

[f]*Kunshan Innovation Institute of Nanjing University, Kunshan, Jiangsu 215347, PR China*

[g] *School of Physics and Engineering, Henan University of Science and Technology, Luoyang 471023, PR China*

[h] *Faculty of Science, King Abdulaziz University, Jeddah 21589, Saudi Aribia*

[i] *Department of Mathematics, Quaid-I-Azam University, Islamabad 45320, Pakistan*

Corresponding Author

*E-mail: ltao84@163.com (T. Li)

*E-mail: guoling.li@gmail.com (G. Li)

*E-mail: zhouyong1999@nju.edu.cn (Y. Zhou)

Experimental section

1.Preparation of $Mo_xCo_{1-x}P$ nanowire array on CC

The Mo_xCo_{1-x}-precursor nanowire array on carbon cloth (CC) were synthesized by hydrothermal reaction. Typically, a piece of CC (1cm×5cm) was carefully pre-treated by concentrated HNO_3 to remove impurity on surface, and cleaned by sonication sequentially in ethanol and deionized water for several times to make sure its surface was cleaned. Then the CC was dried at 60°C for 3 hours. To prepare Co-precursor, $Co(NO_3)_2 \cdot 6H_2O$ (1.5mmol), NH_4F (3mmol) and urea (5mmol) were dissolved in 35mL deionized water with stirring until the solution was clean. Similarly, Mo_xCo_{1-x}-precursor were prepared with the feed ratios of Mo/Co ranging from 0:10, 1:9, 2:8, 3:7 to 4:6 and maintained the total amount of metal atom unchanged (Na_2MoO_4 as the source of Mo). Then the solution was transferred into a 50mL Teflon-lined stainless-steel autoclave and a piece of surface-cleaned CC was immersed into the solution. After heating in an electric oven at 120°C for 6 hours, the CC was taken out and washed by deionized water and ethanol to remove surface impurities and dried overnight.

To synthesize $Mo_xCo_{1-x}P$/CC nanowire array, the as-prepared precursor on CC and 3g NaH_2PO_2 were separated in two different porcelain boats and NaH_2PO_2 was put at the upstream side of the furnace. Then the center of the furnace was heated to 300°C with a rate of 2°C min^{-1} and held at the temperature for 120 minutes.The whole process was finished under a constant Ar flow. Finally, the furnace was naturally cooled down to room temperature with the protection of Ar.

2.Characterization

Powder X-ray diffraction (XRD, RigakuUltimaⅢ, Cu Kα radiation) was used to identify the phase composition of as-synthesized samples. The morphologies were observed by a scanning electron microscope (SEM, Hitachi, S-3400NⅡ), and more detailed morphology information and the elemental composition of the nanowires were examined by a transmission electron microscope (TEM, JEM-200CX). The X-ray photoelectron spectroscopy (XPS) measurements were performed on a PHI 5000

VersaProbe instrument with an Al Kα X-ray radiation.

3.Electrochemical measurements

All electrochemical tests were performedby an electrochemical workstation (CHI660E, Shanghai Chenhua). The synthesized samples were used as working electrode, a graphite rod was utilized as the counter electrode and a saturated calomel electrode (SCE) was served as the reference electrode. All measurements were performedin 1.0M KOH aqueous electrolyte in room temperature. All linear-sweep voltammograms (LSV) were testedat a scan of 2mV s^{-1}, and the potential was converted by the use of equation $E_{RHE}=E_{SCE}+0.244+0.0591\times pH$. The electrochemical impedance spectroscopy (EIS) were carried out at -0.2V (VS SEC) with the sweeping frequency range from 100KHz to 0.1Hz. The stability was testedby controlling potential electrolysis. iR-correction was made to compensate for the voltage drop between the reference and working electrodes by using the equation $E=E_{RHE}-i\times R_S$.

4.Product quantification and Faraday efficiency

The Faraday efficiency of the $Mo_{0.25}Co_{0.75}P$/CC electrocatalyst during the HER was calculated based on the ratio of the amount of hydrogen evolved to the theoretical value.The sample was estimated by a 90 minutes of electrolysis experiment at -0.1V (vs RHE). H_2 gas was collected by an electrolyte drainage method and its amount (mol) was calculated using the ideal gas law.[1,2,3] The theoretical value was calculated according to the Faraday law by assuming the 100% conversion of electron during the electrolysis process.

5. Calculation of turnover number (TON)

The turnover number (TON) of the $Mo_{0.25}Co_{0.75}P$/CC electrocatalyst was estimated after 90 minutes of electrolysis experiment at -0.1V (vs RHE) using the equation as follow:

Turnover number (TON) = [the amount of H_2 evolved / the amount of active centers of the catalyst] [4]

Here we used an electrochemical method to obtain the amount of active centers of the catalyst.[5,6,7]CV curves were tested on the sample in 1M PBS (pH=7) electrolyte.The surface active centers are nearly in linear relationship with the integrated voltammetric chargesbecause there are no obvious redox peaks can be observed.Assuming a one-electron process for both reduction and oxidation,we can evaluate the amount of active centers (n_a) according to the follow formula:

$$n_a = \frac{Q}{2F}$$

Here F and Q correspond to the Faraday constant and the whole charge of CV curve respectively. Thus, we can deduce the amount of active centers of the $Mo_{0.25}Co_{0.75}P$/CC electrocatalyst is close to 1.421×10^{-4}mmol/cm^2. According to the amount of H_2 gas evolvedafter 90 minutes of electrolysis experiment at -0.1V (vs RHE) (0.4692 mmol), we can calculate the TON value to be 3302.

Table S1 Atomic concentration of $Mo_xCo_{1-x}P$

at.%	CoP	$Mo_{0.15}Co_{0.85}P$	$Mo_{0.25}Co_{0.75}P$	$Mo_{0.35}Co_{0.65}P$	$Mo_{0.45}Co_{0.55}P$
C	59.71	94.82	81.29	78.43	90.83
Mo	-	0.32	1.91	3.27	1.83
Co	22.92	2.04	5.97	5.54	2.14
P	17.37	2.82	10.83	12.76	5.20

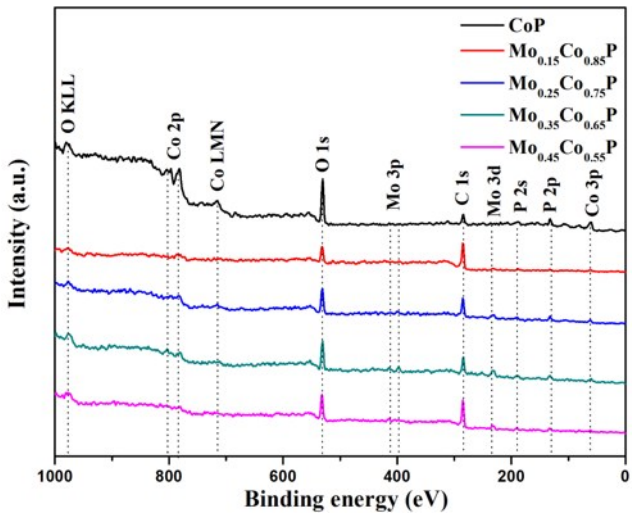

Figure S1 XPS spectrum of $Mo_xCo_{1-x}P$/CC (x=0, 0.15, 0.25, 0.35 and 0.45).

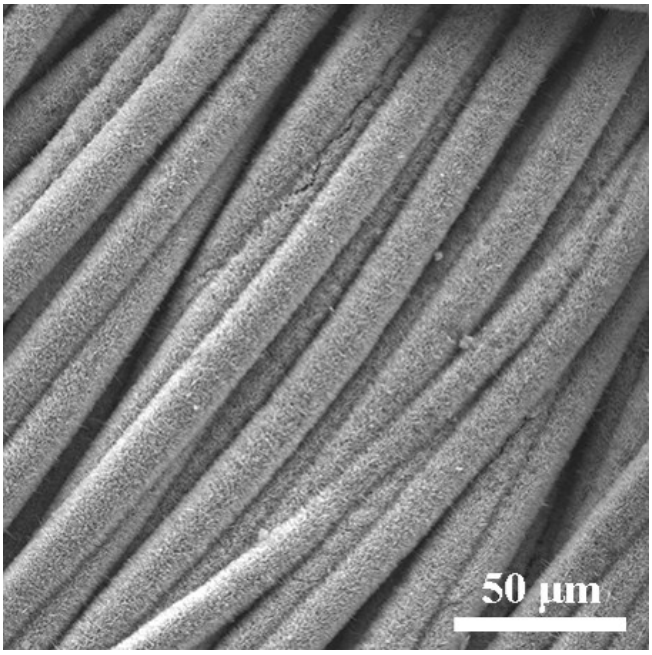

Figure S2 SEM image of $Mo_{0.25}Co_{0.75}P$.

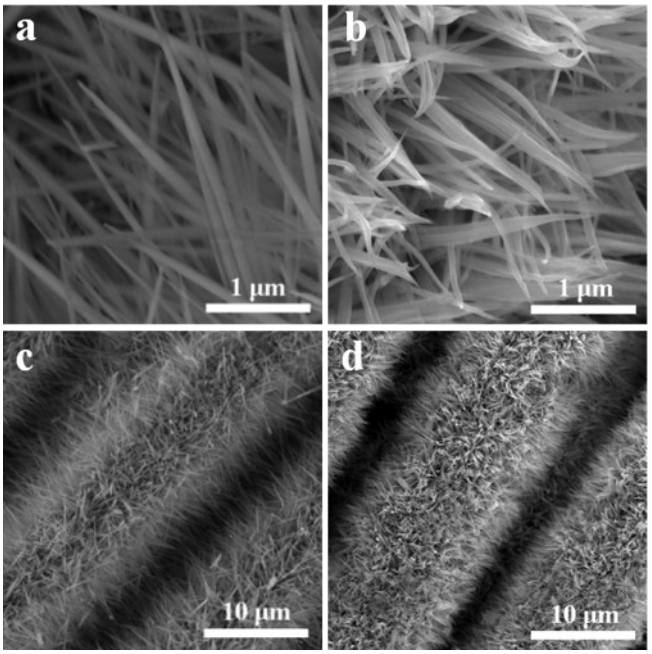

Figure S3 SEM images of (a, c) Co-precursor and (b, d) $Mo_{0.25}Co_{0.75}$-precursor.

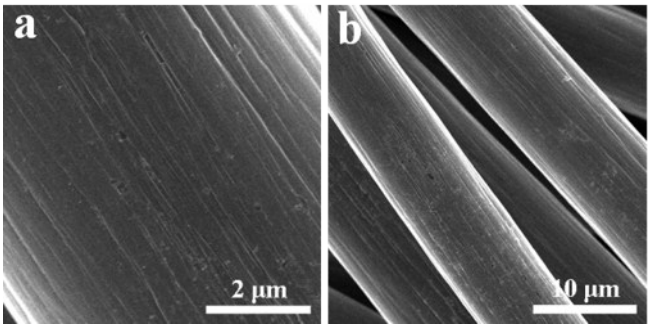

Figure S4 SEM images of bare CC.

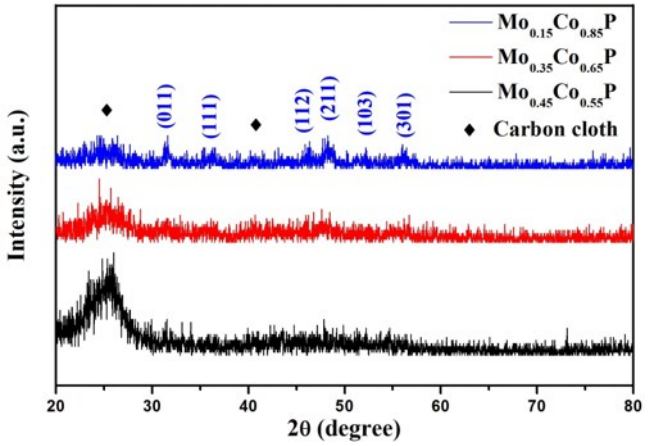

Figure S5 XRD pattern of $Mo_{0.15}Co_{0.85}P$/CC, $Mo_{0.35}Co_{0.65}P$/CC and $Mo_{0.45}Co_{0.55}P$/CC.

Table S2 Comparison of HER performance in alkaline media with other reported ternary non-precious metal TMPs electrocatalysts

Catalysts	$\eta_{10\ mA\ cm^{-2}}$	Tafel slope	Reference
$Mo_{0.25}Co_{0.75}P$/CC	59 mV	52 mV dec^{-1}	This work
$Co_5Mo_{1.0}P$ NSs/NF	173 mV	190.1 mV dec^{-1}	Nano Energy, 2018, 45, 448
$Ni_{0.67}Co_{1.33}P$/N-C NF	130 mV	70 mV dec^{-1}	Applied Catalysis B, 2019,244,620
NiCoP/CC	62 mV	68.2 mV dec^{-1}	ACS Catal., 2017, 7, 4131
NiCoP NSAs	80.9 mV	68.6 mV dec^{-1}	Nano Res., 2016, 9(8), 2251
Ni-FeP/TiN/CC	75 mV	64 mV dec^{-1}	Nano Energy, 2018, 53, 66
Ni-Co-P HNBs	107 mV	46 mV dec^{-1}	Energy Environ. Sci., 2018, 11, 872
Fe-CoP/Ti	78 mV	75 mV dec^{-1}	Adv. Mater., 2017, 29, 1602441
Mn-Co-P/Ti	76 mV	52 mV dec^{-1}	ACS Catal., 2017, 7, 98
Mo-Ni_2P NWs/NF	78 mV	109 mV dec^{-1}	Nanoscale, 2017, 9, 16674
Ni-Co-P	150 mV	60.6 mV dec^{-1}	Chem. Commun., 2016, 52, 1633
Ni_2P/Fe_2P	121 mV	67 mV dec^{-1}	Adv.Energy Mater., 2018, 1800484
CoP/Ni_5P_4/CoP	71 mV	58 mV dec^{-1}	Energy Environ. Sci., 2018, 11, 2246
Ni_2P/Ni_3S_2	80 mV	65 mV dec^{-1}	Nano Energy, 2018, 51, 26
$CoSe_2$|P	104 mV	31 mV dec^{-1}	Nat. Commun. 2018, 9, 2533
S:CoP@NF	109 mV	79 mV dec^{-1}	Nano Energy, 2018, 53, 286

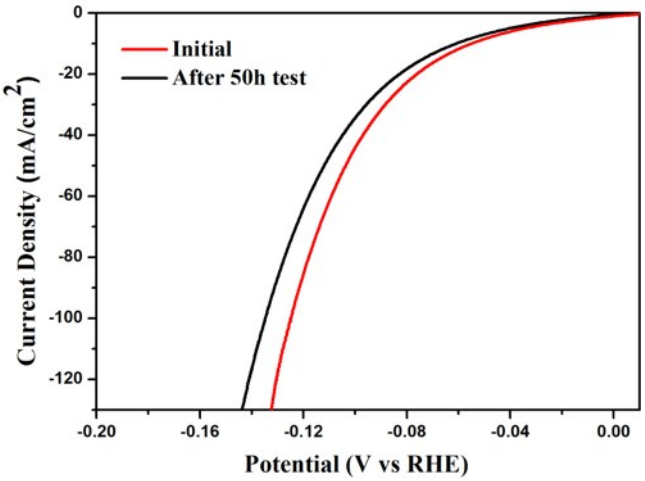

Figure S6. LSV curves for before and after 50h-stability test of $Mo_{0.25}Co_{0.75}P$/CC.

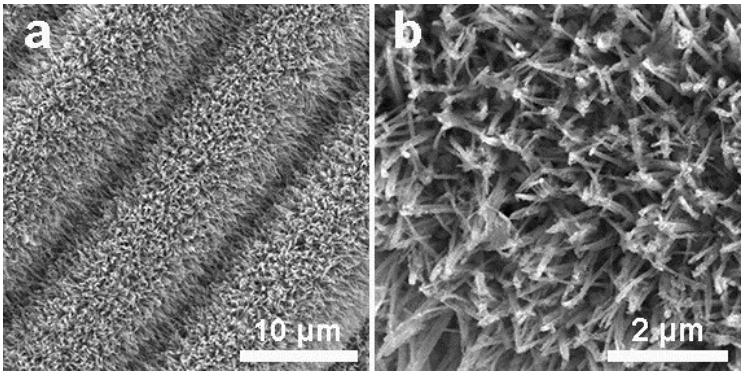

Figure S7. SEM images for $Mo_{0.25}Co_{0.75}P$/CC after durability test. The morphology of nanowires reminds similar to that of $Mo_{0.25}Co_{0.75}P$/CC before test.

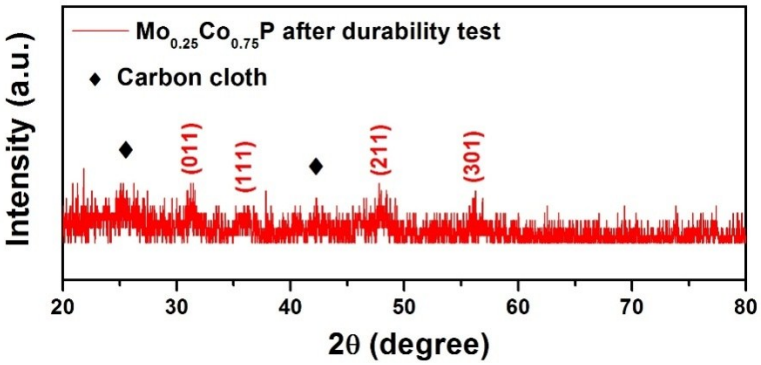

Figure S8. XRDpattern for $Mo_{0.25}Co_{0.75}P$/CC after durability test. The phase composition of nanowires was still retained after test.

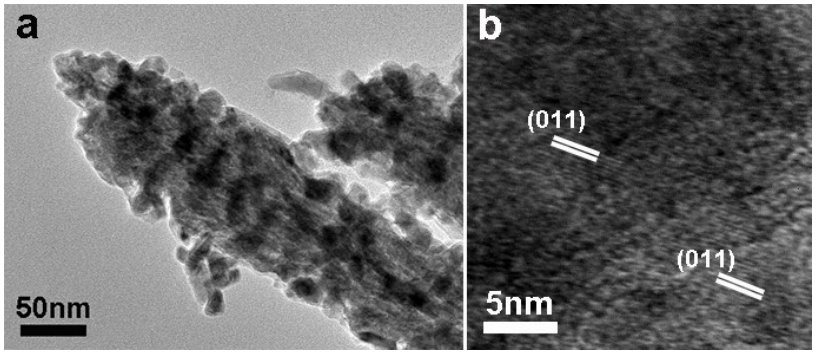

Figure S9. TEM images of $Mo_{0.25}Co_{0.75}P$ after durability test. The morphology and the crystal phase of the nanowire were consistent with the SEM and XRD analyses.

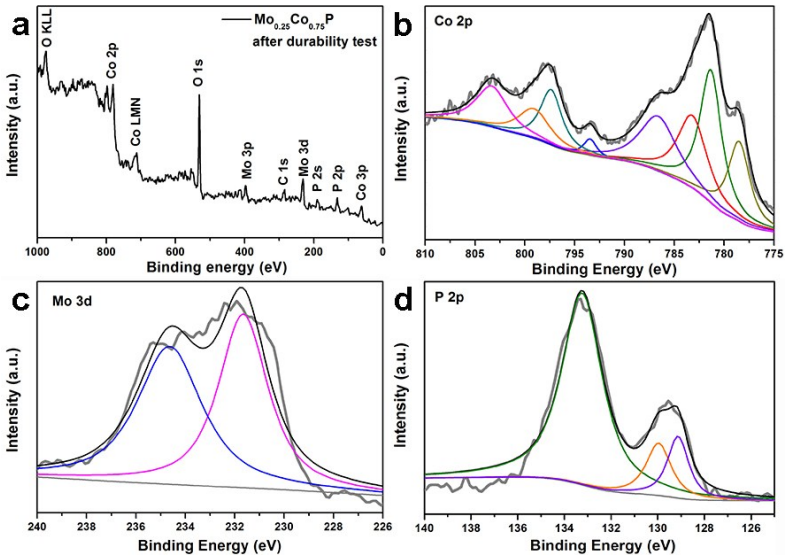

Figure S10. (a) XPSspectrumof $Mo_{0.25}Co_{0.75}P$/CC after durability test and (b) Co 2p, (c) Mo 3d and (d) P 2p.The chemical states of nanowires were still retained after test.

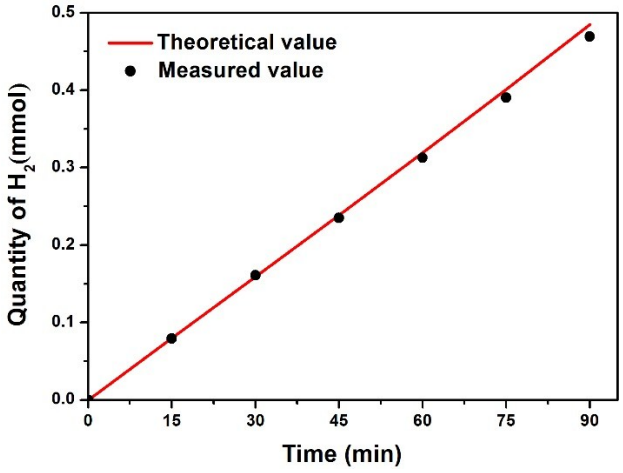

Figure S11. Faraday efficiency of $Mo_{0.25}Co_{0.75}P$/CC for HER.

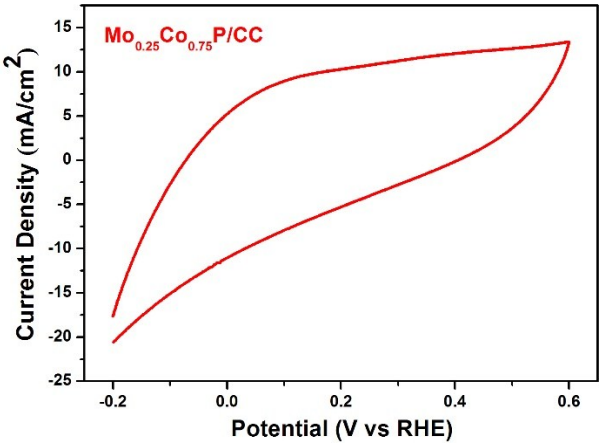

Figure S12. CV curves of $Mo_{0.25}Co_{0.75}P$/CC in 1M PBS (pH=7) with the scan rate of 50 mV s^{-1}.

Computational details:

Density functional theory calculations were done using the projector-augmented wave method and a plane-wave basis set as implemented in the Vienna Ab initio Simulation Package (VASP).[8,9] The valence configurations were treated as $1s^1$ for H, $3s^23p^3$ for P, $3d^84s^1$ for Co, $4d^55s^1$ for Mo, and $5d^96s^1$ for Pt. The Bayesian Error Estimation Functional with van der Waals correlation (BEEF–vdW) was employed.[10] The cutoff energy for plane-wave basis functions was 550 eV. The bulk lattice parameters of CoP and Pt were fully optimized based on experimental data (CoP PDF#29-0497, Pt PDF# 4-802). By substituting Co atoms with Mo atoms within 16-atoms supercells of CoP, the bulk structures of $Mo_xCo_{1-x}P$ (x = 0.125, 0.250, 0.375, 0.500) were generated via the Special Quasirandom Structures (SQS) method, which has been widely used to determine the atomic distributions in solid solutions.[11] Based on the optimized structural parameters, we constructed periodic surface slabs including (100), (010), (001), (110), (101), (011), (111) for CoP, (011) and (101) for $Mo_xCo_{1-x}P$, and (111) for Pt. In construction of the surface slabs of CoP, both Co and P terminations were carefully considered. For periodic slab calculations, slabs of six to ten Co/Mo or Pt layers were separated by at least 16 Å of vacuum. All atomic positions of the slabs were allowed to relax in surface energy calculations, and only atomic positions within

the top three layers of the slabs were allowed to relax in hydrogen binding energy calculations. All calculations were done in Γ-centered Monkhorst–Pack *k*-point meshes with a reciprocal-space resolution of 0.15 Å^{-1}. The energy convergence was 10^{-5} eV and the force convergence 0.01 eV/Å.

The surface energy σis defined as $\sigma = (E_{slab}-E_{bulk})/2A$, where E_{slab} is the total energy of the relaxed slab, E_{bulk} the total energy of the bulk, and A the area of surface unit cell.[12]The equilibrium morphology of CoP is determined from the calculated surface energies via Wulff construction.[12]

As is known, catalytic activity of the material is determined by the binding energies of the reaction intermediates to the active sites of the catalyst. In the hydrogen evolution reaction, only H* intermediate is involved. To estimate the free energies of hydrogen adsorption ΔG_H at zero potential and pH = 0, we calculated the binding energies ΔE_H of H* intermediate and corrected them with zero point energy (ZPE) and entropy (TS) using $\Delta G_H = \Delta E_H + \Delta ZPE - T\Delta S$.[6]Here, ΔE_H and ΔG_H are calculated with respect to H_2(g).

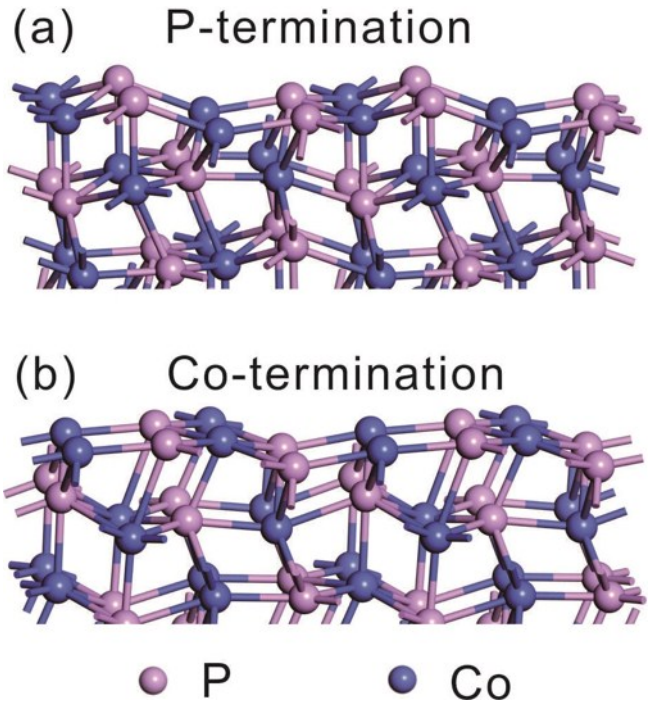

Figure S13 Side view of the relaxed geometric structures of the 2×2 CoP (101) surface terminated with (a) phosphorus and (b) cobalt.

Table S3. The calculated surface energy σ for low-index surfaces of CoP and the corresponding facets' contribution γ to total surface region of the equilibrium morphology.

Surface	(100)	(010)	(001)	(110)	(101)	(011)	(111)
σ (J/m^2)	2.03	1.55	1.53	1.75	1.33	1.11	1.42
γ (%)	0.00	3.63	0.00	0.00	25.24	46.52	24.61

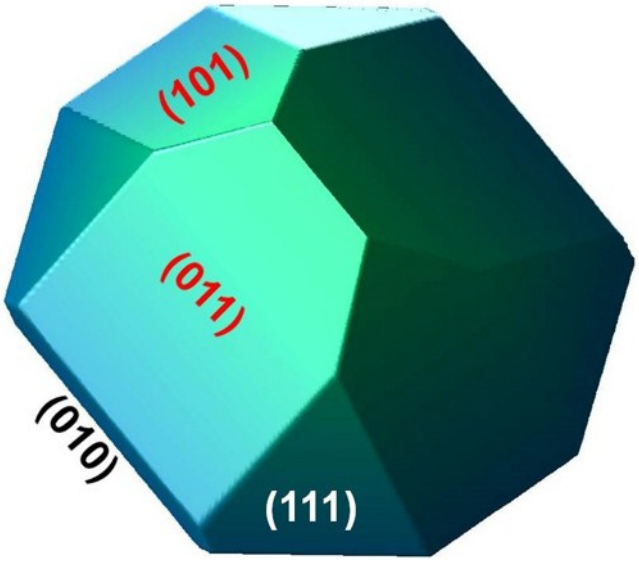

Figure S14. Equilibrium morphology of CoP.

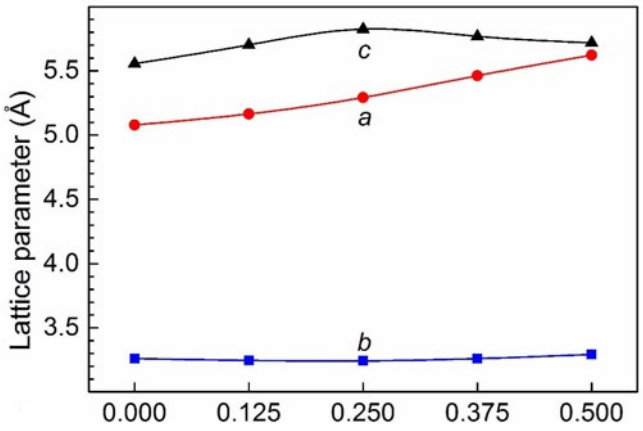

Figure S15. The calculated lattice parameters *a*, *b*, and *c* of bulk $Mo_xCo_{1-x}P$.

Reference

(1) Q. Zhou, Z. Shen, C. Zhu, J. Li, Z. Ding, P. Wang, F. Pan, Z. Zhang, H. Ma, S. Wang and H. Zhang, *Adv. Mater.*, 2018, **30**, 1800140.

(2) Q. Zhou, J. Pu, X. Sun, C. Zhu, J. Li, J. Wang, S. Chang and H. Zhang, *J. Mater. Chem. A*, 2017, **5**, 14873.

(3) Y. Liu, Q. Li, R. Si, G.-D. Li, W. Li, D.-P. Liu, D. Wang, L. Sun, Y. Zhang and X. Zou, *Adv. Mater.*, 2017, **29**, 1606200.

(4) B. C. Patra, S. Khilari, R. N. Manna, S. Mondal, D. Pradhan, A. Pradhan and A. Bhaumik, *ACS Catal.,* 2017, **7**, 6120-6127.

(5) I. K. Mishra, H. Zhou, J. Sun, F. Qin, K. Dahal, J. Bao, S. Chen and Z. Ren, *Energy Environ. Sci.*, 2018, **11**, 2246-2252.

(6) J. Xu, T. Liu, J. Li, Y. Liu, B. Zhang, D. Xiong, I. Amorim and W. Li, L. Liu, *Energy Environ. Sci.*, 2018, **11**, 1819-1827.

(7) X. Dai, K. Du, Z. Li, M. Liu, Y. Ma, H. Sun, X. Zhang and Y. Yang, *ACS Appl. Mater. Interface*, 2015, **7**, 27242-27253.

(8) Blöchl, P.E. Projector augmented-wave method, *Phys. Rev. B*,**50**, 17953–17979.

(9) Kresse, G. andFurthmüller, J., *Phys. Rev. B,*1996, **54**, 11169–11186.

(10) Wellendorff, J., Lundgaard, K.T., Møgelhøj, A., Petzold, V., Landis, D.D., Nørskov, J.K., Bligaard, T. and Jacobsen, K.W. Density functionals for surface science: exchange-correlation model development with Bayesian error estimation, *Phys Rev B*2012,**85**, 235149.

(11) Wei, S.-H., Ferreira, L.G., Bernard, J.E. andZunger, A. Electronic properties of random alloys: Special quasirandom structures, *Phys. Rev.B*1990, **42**, 9622–9649.

(12) Li, G.-L. First-principles investigation of the surface properties of fergusonite-type monoclinic $BiVO_4$photocatalyst, *RSC Adv.*2017, **7**, 9130-9140.

(13) Norskov, J.K., Rossmeisl J., Logadottir, A., Lindqvist, L., Kitchin, J.R., Bligaard, T. &Jonsson, H., Origin of the Overpotential for Oxygen Reduction at a Fuel Cell

Cathode, *J. Phys. Chem. B*2004, **108**, 17886-17892.